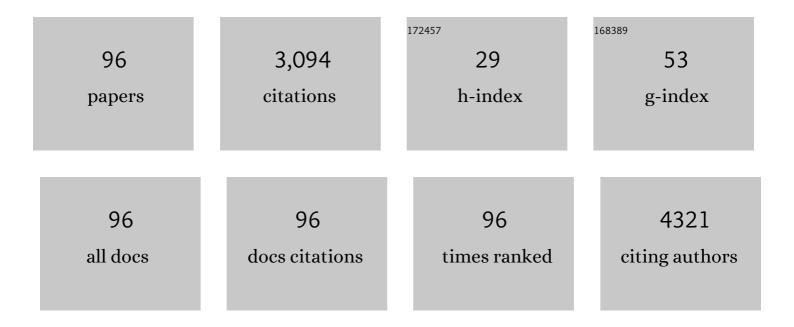
Andrew H A Clayton

List of Publications by Year in descending order

Source: https://exaly.com/author-pdf/5354550/publications.pdf Version: 2024-02-01



#	Article	IF	CITATIONS
1	Red-Edge Excitation Shift Spectroscopy (REES): Application to Hidden Bound States of Ligands in Protein–Ligand Complexes. International Journal of Molecular Sciences, 2021, 22, 2582.	4.1	6
2	Dynamic Cellular Cartography: Mapping the Local Determinants of Oligodendrocyte Transcription Factor 2 (OLIG2) Function in Live Cells Using Massively Parallel Fluorescence Correlation Spectroscopy Integrated with Fluorescence Lifetime Imaging Microscopy (mpFCS/FLIM). Analytical Chemistry, 2021, 93, 12011-12021.	6.5	8
3	Uptake quantification of gold nanoparticles inside of cancer cells using high order image correlation spectroscopy. Biomedical Optics Express, 2021, 12, 539.	2.9	5
4	In-cell structural dynamics of an EGF receptor during ligand-induced dimer–oligomer transition. European Biophysics Journal, 2020, 49, 21-37.	2.2	6
5	Using fluorescence lifetime dequenching to estimate the average quinary stoichiometry of proteins in living cells. Methods and Applications in Fluorescence, 2020, 8, 014003.	2.3	1
6	Effects of Rationally Designed Physico-Chemical Variants of the Peptide PuroA on Biocidal Activity towards Bacterial and Mammalian Cells. International Journal of Molecular Sciences, 2020, 21, 8624.	4.1	8
7	Deducing the Conformational Properties of a Tyrosine Kinase Inhibitor in Solution by Optical Spectroscopy and Computational Chemistry. Frontiers in Chemistry, 2020, 8, 596.	3.6	4
8	Does frequency-dependent cell proliferation exhibit a Fano-type resonance?. Physical Biology, 2020, 17, 044001.	1.8	1
9	Plasmon-induced photoluminescence and Raman enhancement in Pr:CaF2 crystal by embedded silver nanoparticles. Applied Surface Science, 2020, 530, 147018.	6.1	11
10	Spectroscopic and Microscopic Approaches for Investigating the Dynamic Interactions of Anti-microbial Peptides With Membranes and Cells. Frontiers in Medical Technology, 2020, 2, 628552.	2.5	0
11	Structural and Spectroscopic Study of the Tyrosine Kinase Inhibitor PD-153035. Biophysical Journal, 2019, 116, 568a.	0.5	0
12	pbICS microscopy technique for determining oligomeric state. , 2019, , .		1
13	Conformational Plasticity in Tyrosine Kinase Inhibitor–Kinase Interactions Revealed with Fluorescence Spectroscopy and Theoretical Calculations. Journal of Physical Chemistry B, 2018, 122, 4667-4679.	2.6	7
14	Antimicrobial peptides: biochemical determinants of activity and biophysical techniques of elucidating their functionality. World Journal of Microbiology and Biotechnology, 2018, 34, 62.	3.6	28
15	Exploring oligomeric state of the serotonin _{1A} receptor utilizing photobleaching image correlation spectroscopy: implications for receptor function. Faraday Discussions, 2018, 207, 409-421.	3.2	20
16	The Effect of Nanoparticles on the Cluster Size Distributions of Activated EGFR Measured with Photobleaching Image Correlation Spectroscopy. Advances in Experimental Medicine and Biology, 2018, 1112, 41-52.	1.6	2
17	The architecture of EGFR's basal complexes reveals autoinhibition mechanisms in dimers and oligomers. Nature Communications, 2018, 9, 4325.	12.8	71
18	Fluorescence-based approaches for monitoring membrane receptor oligomerization. Journal of Biosciences, 2018, 43, 463-469.	1.1	6

#	Article	IF	CITATIONS
19	Confocal Microscopy Reveals Cell Surface Receptor Aggregation Through Image Correlation Spectroscopy. Journal of Visualized Experiments, 2018, , .	0.3	3
20	Revealing the sequence of interactions of PuroA peptide with Candida albicans cells by live-cell imaging. Scientific Reports, 2017, 7, 43542.	3.3	21
21	Exploring the optical reporting characteristics of drugs: UV-Vis spectra and conformations of the tyrosine kinase inhibitor SKF86002. New Journal of Chemistry, 2017, 41, 14567-14573.	2.8	4
22	Micro-solvation of tyrosine-kinase inhibitor AG1478 explored with fluorescence spectroscopy and computational chemistry. RSC Advances, 2017, 7, 31725-31735.	3.6	5
23	Multidimensional Microscopy: Application to Membrane Protein Structure. Springer Series in Biophysics, 2017, , 91-111.	0.4	Ο
24	Solvatochromism and linear solvation energy relationship of the kinase inhibitor SKF86002. Spectrochimica Acta - Part A: Molecular and Biomolecular Spectroscopy, 2017, 170, 226-233.	3.9	4
25	A pH-induced conformational switch in a tyrosine kinase inhibitor identified by electronic spectroscopy and quantum chemical calculations. Scientific Reports, 2017, 7, 16271.	3.3	3
26	Anti-biofilm and sporicidal activity of peptides based on wheat puroindoline and barley hordoindoline proteins. Journal of Peptide Science, 2016, 22, 492-500.	1.4	32
27	Analysis of complex anisotropy decays from single-frequency polarized-phasor ellipse plots. Methods and Applications in Fluorescence, 2016, 4, 024005.	2.3	3
28	UV–Vis spectroscopy and solvatochromism of the tyrosine kinase inhibitor AG-1478. Spectrochimica Acta - Part A: Molecular and Biomolecular Spectroscopy, 2016, 164, 128-132.	3.9	14
29	Interactions of a lytic peptide with supported lipid bilayers investigated by time-resolved evanescent wave-induced fluorescence spectroscopy. Methods and Applications in Fluorescence, 2016, 4, 044001.	2.3	2
30	Two conformers of a tyrosine kinase inhibitor (AG-1478) disclosed using simulated UV-Vis absorption spectroscopy. New Journal of Chemistry, 2016, 40, 8296-8304.	2.8	16
31	EGFR oligomerization organizes kinase-active dimers into competent signalling platforms. Nature Communications, 2016, 7, 13307.	12.8	146
32	Imaging Cellular Dynamics with Spectral Relaxation Imaging Microscopy: Distinct Spectral Dynamics in Golgi Membranes of Living Cells. Scientific Reports, 2016, 6, 37038.	3.3	13
33	Direct Measurement of Pore Dynamics and Leakage Induced by a Model Antimicrobial Peptide in Single Vesicles and Cells. Langmuir, 2016, 32, 6496-6505.	3.5	6
34	BioNetFit: a fitting tool compatible with BioNetGen, NFsim and distributed computing environments. Bioinformatics, 2016, 32, 798-800.	4.1	31
35	Spatiotemporal Control of Transmembrane Proteins through the Cytoskeleton: AnÂEvolving Story. Biophysical Journal, 2016, 110, 1036-1037.	0.5	1
36	Archetypal tryptophan-rich antimicrobial peptides: properties and applications. World Journal of Microbiology and Biotechnology, 2016, 32, 31.	3.6	67

#	Article	IF	CITATIONS
37	Gold Nanoparticles: Inhibiting EGFR Clustering and Cell Proliferation with Gold Nanoparticles (Small) Tj ETQq1	0.784314	rgBT /Overlo
38	Deep-UV fluorescence lifetime imaging microscopy. Photonics Research, 2015, 3, 283.	7.0	11
39	The transition from single molecule to ensemble revealed by fluorescence polarization Scientific Reports, 2015, 5, 8158.	3.3	5
40	Inhibiting EGFR Clustering and Cell Proliferation with Gold Nanoparticles. Small, 2015, 11, 1638-1643.	10.0	17
41	Polarization of excitation light influences molecule counting in single-molecule localization microscopy. Histochemistry and Cell Biology, 2015, 143, 11-19.	1.7	6
42	SpIDA Surveys the Intricate Web of Macromolecular Oligomerization In Situ. Biophysical Journal, 2015, 109, 663-664.	0.5	0
43	Get Your kICS by Measuring Membrane Protein Dynamics. Biophysical Journal, 2015, 109, 1-2.	0.5	18
44	Determining complex aggregate distributions of macromolecules using photobleaching image correlation microscopy. AIMS Biophysics, 2015, 2, 1-7.	0.6	5
45	A Microfluidic Device for Spatiotemporal Delivery of Stimuli to Cells. AIMS Biophysics, 2015, 2, 58-72.	0.6	2
46	Recruitment of the Adaptor Protein Grb2 to EGFR Tetramers. Biochemistry, 2014, 53, 2594-2604.	2.5	36
47	Taking Care of Bystander FRET in a Crowded Cell Membrane Environment. Biophysical Journal, 2014, 106, 1227-1228.	0.5	18
48	Solvent Relaxation in Golgi Membrane by Phasor-Flim Approach. Biophysical Journal, 2014, 106, 204a.	0.5	0
49	Cell Surface Receptors in the 21st Century. AIMS Biophysics, 2014, 1, 51-52.	0.6	1
50	The Effect of Translational Motion on FLIM Measurements-Single Particle Phasor-FLIM. Journal of Fluorescence, 2013, 23, 671-679.	2.5	1
51	Exploring higher-order EGFR oligomerisation and phosphorylation—a combined experimental and theoretical approach. Molecular BioSystems, 2013, 9, 1849.	2.9	72
52	Characterization of optical polarization converters made by femtosecond laser writing. , 2013, , .		0
53	Temperature measurement in the microscopic regime: a comparison between fluorescence lifetime―and intensityâ€based methods. Journal of Microscopy, 2013, 250, 179-188.	1.8	38
54	A Toolbox of Fluorescence Microscopic Approaches Reveals Dynamics and Assembly of a Membrane-Associated Protein. Biophysical Journal, 2013, 104, 1844-1845.	0.5	1

#	Article	IF	CITATIONS
55	Aggregation Distributions on Cells Determined by Photobleaching Image Correlation Spectroscopy. Biophysical Journal, 2013, 104, 1056-1064.	0.5	26
56	Imaging the action of antimicrobial peptides on living bacterial cells. Scientific Reports, 2013, 3, 1557.	3.3	69
57	Long-Time-Scale Interaction Dynamics between a Model Antimicrobial Peptide and Giant Unilamellar Vesicles. Langmuir, 2013, 29, 14613-14621.	3.5	9
58	A microfluidic device for studying cell signaling with multiple inputs and adjustable amplitudes and frequencies. Proceedings of SPIE, 2013, , .	0.8	0
59	Ultra-pure, water-dispersed Au nanoparticles produced by femtosecond laser ablation and fragmentation. International Journal of Nanomedicine, 2013, 8, 2601.	6.7	19
60	Ligand binding induces a conformational change in epidermal growth factor receptor dimers. Growth Factors, 2012, 30, 394-409.	1.7	20
61	Slow Insertion Kinetics during Interaction of a Model Antimicrobial Peptide with Unilamellar Phospholipid Vesicles. Langmuir, 2012, 28, 2217-2224.	3.5	21
62	Regulation of Actin Dynamics by Protein Kinase R Control of Gelsolin Enforces Basal Innate Immune Defense. Immunity, 2012, 36, 795-806.	14.3	54
63	The influence of nanostructured materials on biointerfacial interactions. Advanced Drug Delivery Reviews, 2012, 64, 1820-1839.	13.7	108
64	Targeting of a Conformationally Exposed, Tumor-Specific Epitope of EGFR as a Strategy for Cancer Therapy. Cancer Research, 2012, 72, 2924-2930.	0.9	124
65	Conformational Dynamics in a Truncated Epidermal Growth Factor Receptor Ectodomain. Biochemistry, 2011, 50, 5130-5139.	2.5	6
66	Organization of Higher-Order Oligomers of the Serotonin1A Receptor Explored Utilizing Homo-FRET in Live Cells. Biophysical Journal, 2011, 100, 361-368.	0.5	95
67	Structural Dynamics of a Lytic Peptide Interacting with a Supported Lipid Bilayer. Biophysical Journal, 2011, 100, 1353-1361.	0.5	22
68	Fixation alters fluorescence lifetime and anisotropy of cells expressing EYFP-tagged serotonin1A receptor. Biochemical and Biophysical Research Communications, 2011, 405, 234-237.	2.1	23
69	Differential and Synergistic Effects of Epidermal Growth Factor Receptor Antibodies on Unliganded ErbB Dimers and Oligomers. Biochemistry, 2011, 50, 3581-3590.	2.5	15
70	Evidence for extended YFP-EGFR dimers in the absence of ligand on the surface of living cells. Physical Biology, 2011, 8, 066002.	1.8	27
71	Creation and Biophysical Characterization of a High-Affinity, Monomeric EGF Receptor Ectodomain Using Fluorescent Proteins. Biochemistry, 2010, 49, 7459-7466.	2.5	4
72	Antibodies specifically targeting a locally misfolded region of tumor associated EGFR. Proceedings of the United States of America, 2009, 106, 5082-5087.	7.1	69

#	Article	IF	CITATIONS
73	The Preparation of Colloidally Stable, Water-Soluble, Biocompatible, Semiconductor Nanocrystals with a Small Hydrodynamic Diameter. ACS Nano, 2009, 3, 1121-1128.	14.6	171
74	Profilin Interaction with Phosphatidylinositol (4,5)-Bisphosphate Destabilizes the Membrane of Giant Unilamellar Vesicles. Biophysical Journal, 2009, 96, 5112-5121.	0.5	22
75	Recruitment of adenomatous polyposis coli and β-catenin to axin-puncta. Oncogene, 2008, 27, 5808-5820.	5.9	63
76	The polarized AB plot for the frequencyâ€domain analysis and representation of fluorophore rotation and resonance energy homotransfer. Journal of Microscopy, 2008, 232, 306-312.	1.8	22
77	Predominance of activated EGFR higher-order oligomers on the cell surface. Growth Factors, 2008, 26, 316-324.	1.7	77
78	Experimental Determination of Quantum Dot Size Distributions, Ligand Packing Densities, and Bioconjugation Using Analytical Ultracentrifugation. Nano Letters, 2008, 8, 2883-2890.	9.1	95
79	Unligated Epidermal Growth Factor Receptor Forms Higher Order Oligomers within Microclusters on A431 Cells That Are Sensitive to Tyrosine Kinase Inhibitor Binding. Biochemistry, 2007, 46, 4589-4597.	2.5	76
80	Enumeration of Oligomerization States of Membrane Proteins in Living Cells by Homo-FRET Spectroscopy and Microscopy: Theory and Application. Biophysical Journal, 2007, 92, 3098-3104.	0.5	91
81	Fluorescence and analytical ultracentrifugation analyses of the interaction of the tyrosine kinase inhibitor, tyrphostin AG1478-mesylate, with albumin. Analytical Biochemistry, 2005, 342, 292-299.	2.4	8
82	Dual-channel photobleaching FRET microscopy for improved resolution of protein association states in living cells. European Biophysics Journal, 2005, 34, 82-90.	2.2	16
83	Ligand-induced Dimer-Tetramer Transition during the Activation of the Cell Surface Epidermal Growth Factor Receptor-A Multidimensional Microscopy Analysis. Journal of Biological Chemistry, 2005, 280, 30392-30399.	3.4	232
84	Defective Calmodulin-Mediated Nuclear Transport of the Sex-Determining Region of the Y Chromosome (SRY) in XY Sex Reversal. Molecular Endocrinology, 2005, 19, 1884-1892.	3.7	52
85	Unfolding of Class A Amphipathic Peptides on a Lipid Surfaceâ€. Biochemistry, 2003, 42, 1747-1753.	2.5	3
86	A SOX9 Defect of Calmodulin-dependent Nuclear Import in Campomelic Dysplasia/Autosomal Sex Reversal. Journal of Biological Chemistry, 2003, 278, 33839-33847.	3.4	99
87	Dynamic Fluorescence Anisotropy Imaging Microscopy inthe Frequency Domain (rFLIM). Biophysical Journal, 2002, 83, 1631-1649.	0.5	201
88	Site-specific tryptophan fluorescence spectroscopy as a probe of membrane peptide structure and dynamics. European Biophysics Journal, 2002, 31, 9-13.	2.2	34
89	Compound Effects of Point Mutations Causing Campomelic Dysplasia/Autosomal Sex Reversal upon SOX9 Structure, Nuclear Transport, DNA Binding, and Transcriptional Activation. Journal of Biological Chemistry, 2001, 276, 27864-27872.	3.4	84
90	Site-Specific Tryptophan Dynamics in Class A Amphipathic Helical Peptides at a Phospholipid Bilayer Interface. Biophysical Journal, 2000, 79, 1066-1073.	0.5	21

#	Article	IF	CITATIONS
91	The structure and orientation of class-A amphipathic peptides on a phospholipid bilayer surface. European Biophysics Journal, 1999, 28, 133-141.	2.2	31
92	Tryptophan Rotamer Distributions in Amphipathic Peptides at a Lipid Surface. Biophysical Journal, 1999, 76, 3235-3242.	0.5	56
93	Helixâ^'Helix Association of a Lipid-Bound Amphipathic α-Helix Derived from Apolipoprotein C-llâ€. Biochemistry, 1999, 38, 10878-10884.	2.5	25
94	Through-Bond and Through-Space Coupling in Photoinduced Electron and Energy Transfer:Â AnabInitioand Semiempirical Study. The Journal of Physical Chemistry, 1996, 100, 10912-10918.	2.9	77
95	On the rate of radiationless intermolecular energy transfer. Journal of Chemical Physics, 1992, 97, 7405-7413.	3.0	39
96	Optical spectra and conformation pool of tyrosine kinase inhibitor PD153035 using a robust quantum mechanical conformation search. New Journal of Chemistry, 0, , .	2.8	1